Geochronology of Taung and other southern African australopiths

Pieter Vermeesch
University College London, Gower Street
London WC1E 6BT
p.vermeesch [at] ucl.ac.uk

Philip Hopley
Birkbeck, University of London, Malet Street
London WC1E 7HX
p.hopley [at] ucl.ac.uk

Nick Roberts
British Geological Survey, Keyworth
Nottingham NG12 5GG
nirob [at] bgs.ac.uk

Randall Parrish
University of Portsmouth
Portsmouth PO1 3QL
randall.parrish [at] port.ac.uk

January 29, 2025

Abstract

One century after the Taung juvenile's discovery, its age and that of many other southern African australopiths remains unknown. This lack of accurate geochronological constraints leaves important questions unanswered, including the temporal relationship between the South African fossil sites and their well dated eastern African counterparts. Previous age estimates for the Taung fossil range from 942 ka to 3.03 Ma. Radiometric age estimation is difficult in the absence of the volcanic marker beds that are so useful in eastern Africa. The advent of carbonate U–Pb geochronology has been heralded as the long-awaited solution to this conundrum. However, some notes of caution are necessary, because the $^{206}Pb/^{238}U$ isochron method requires correction for any initial $^{234}U/^{238}U$ disequilibrium. In the case of southern African carbonates, this correction sometimes exceeds 50%. We show that, beyond ~ 1.5 Ma, the uncertainty of the disequilibrium correction may exceed the correction itself, degrading the value of the $^{206}Pb/^{238}U$ method. We propose the $^{207}Pb/^{235}U$ method as an alternative to the $^{206}Pb/^{238}U$ method, because it is largely unaffected by initial disequilibrium. We use this alternative U–Pb dating approach to obtain a new minimum age estimate for the Taung juvenile, by analysing a flowstone situated above, and in stratigraphic succession with, the fossil-bearing deposit. The uncorrected $^{206}Pb/^{238}U$ isochron age for the sample is 3.30 ± 0.12 Ma. Disequilibrium correction lowers this value to $2.05 + 0.11/-0.08$ Ma, a correction of 40%. The $^{207}Pb/^{235}U$ isochron age of 2.982 ± 0.057 Ma is close to the uncorrected $^{206}Pb/^{238}U$ age. Unfortunately, the two age

estimates do not overlap within uncertainty. We attribute this disagreement to open system behaviour of the uranium in the sample, which leads to an overestimation of the $^{234}U/^{238}U$ disequilibrium correction and an underestimation of the $^{207}Pb/^{235}U$ isochron age. Consequently, the $^{207}Pb/^{235}U$ isochron age of ~ 3 Ma is a minimum age estimate for the flowstone and for the Taung juvenile, placing both firmly in the Pliocene epoch. Disappointingly, LA-ICP-MS screening of borehole samples below the Taung discovery site have not yielded any further datable carbonates. Therefore, we have not been able to pair our minimum age estimate with an equally robust upper age bracket. The search for this additional age constraint continues.

1 Introduction

The scientific importance of the Taung juvenile (hereafter Taung) can hardly be overstated. It is the holotype of *Australopithecus africanus* and provided the first evidence for Charles Darwin's assertion that humans evolved in Africa (Dart, 1925). But despite its importance and 100 years of research, the age of the fossil is frustratingly poorly constrained. This is due to a combination of at least five reasons:

The Plio-Pleistocene geochronology conundrum. The Plio-Pleistocene falls in an awkward 'dating gap' between young events (< 50 ka) that can be dated with radiocarbon, and older parts of the geologic timescale (> 5 Ma), where long-lived radionuclides such as ^{238}U and ^{40}K can be routinely used (Isaac, 1975).

Nevertheless, the burgeoning field of Quaternary geochronology has produced a number of breakthrough technologies that generate robust Plio-Pleistocene age constraints. Arguably the most successful of these techniques is $^{40}Ar/^{39}Ar$-dating of volcanic ash. This method has provided precise and accurate time constraints on human evolution in eastern Africa (Deino et al., 2023). Unfortunately, it is not applicable to southern Africa, for reasons we discuss.

Geological setting. Famous eastern African hominin discovery sites, such as the Omo-Turkana Basin and Olduvai (now Oldupai), are situated in the eastern African rift system (EARS), an area of active volcanism. This geological setting creates the ideal conditions for accurate chronostratigraphy. Many eastern African hominin fossils are found in fluviolacustrine deposits intercalated with volcanic ash layers amenable to K–Ar and $^{40}Ar/^{39}Ar$ dating (Leakey et al., 1961; Deino et al., 2023).

Unfortunately, the EARS terminates in Malawi and no recent volcanic activity is found south of that. Therefore, the $^{40}Ar/^{39}Ar$ method is not applicable to southern African hominins and other, less straightforward techniques must be used.

Whereas eastern African hominin fossils are generally found in siliciclastic deposits, many southern African specimens were discovered in carbonate lithologies (caves and tufa deposits). Until recently, the two dominant techniques to determine the age of these rocks were terrestrial cosmogenic nuclide (TCN) geochronology of siliciclastic cave fill (e.g., Partridge et al., 2003; Granger et al., 2015; Kramers and Dirks, 2017; Granger et al., 2022) and Th/U disequilibrium dating of speleothems, or of the fossils themselves (e.g., Vogel and Partridge, 1984; Grün and Stringer, 2023). The Th/U disequilibrium dating method has an age limit of ~ 500 ka and is sensitive to U-migration, which can be triggered by changes in redox state (Tobias et al., 1993; Ivanovich, 1994). In recent years, the carbonate U–Pb method has gained significant popularity as a replacement for TCN and Th/U disequilibrium dating (Walker et al., 2006; Dirks et al., 2010; Pickering et al., 2019).

Inconsistent results. Unfortunately, the U–Pb results are inconsistent with previously obtained TCN dates. Whereas the TCN dates of southern African australopiths are similar to the

ages of their eastern African counterparts, their U–Pb dates are systematically younger by ∼1 Ma (Section 2). Complex sedimentological arguments have been developed to reconcile these differences, either by arguing that the cosmogenic nuclide dates are too old (Kramers and Dirks, 2017), or that the U–Pb dates are too young (Bruxelles et al., 2019; Granger et al., 2022).

Unknown discovery location. The previous three problems apply to all southern African hominins. The situation is further complicated for Taung because the exact location of its discovery is unknown. The skull was found by a quarry worker ('Mr. de Bruyn'; Tobias, 1984, 2000) in the Buxton-Norlim limeworks. By the time its scientific value was recognised, the quarrying had progressed beyond the discovery site. Quarrying continued until until the 1970s, removing most geological evidence except for two 'pinnacles' that were left standing near the discovery site thanks to the foresight of the quarry manager.

These pinnacles were named after Raymond Dart (the anatomist who recognised that Taung was a hominin and not a baboon) and Aleš Hrdlička (who carried out an early expedition to Taung in 1925). Our current understanding of the Taung stratigraphy is mostly based on the Dart and Hrdlička pinnacles and the shallow subsurface beneath them.

Geographic isolation. In the absence of reliable radiometric age constraints, biostratigraphic correlations with other hominin discovery sites offer an alternative approach to constraining geologic time. Unfortunately, such correlations are difficult for Taung, not only because its stratigraphic context is poorly preserved (see the previous point), but also because the site is geographically isolated from other hominin discovery sites. Taung is located near the edge of the Kalahari desert in the present day and it experiences more arid conditions than the Cradle of Humankind. If similar climatic and ecological gradients were present in the Plio-Pleistocene, they may complicate biological correlations between these two regions (McKee, 1993).

The coincidence of the above five problems explains why the age of Taung is so poorly constrained, with estimates ranging from 1 to 3 Ma. Section 3 will review these existing estimates and will explain in more detail why none of them are entirely reliable. Section 4 will review the carbonate U–Pb dating method, which has been proposed as a potential solution to the southern African hominin dating conundrum (Woodhead and Pickering, 2012). We will show that this technique has issues of its own, which lead us to conclude that the accuracy and precision of several published hominin dates has been overestimated.

Fortunately, there is hope for a better solution. Section 5 will advocate the $^{207}Pb/^{235}U$ method as a more accurate approach to U–Pb geochronology than the established $^{206}Pb/^{238}U$ method. We will use this new flavour of U–Pb geochronology to obtain a robust minimum age estimate for Taung of ~ 3 Ma. The new estimate is considerably older than the disequilibrium-corrected $^{206}Pb/^{238}U$ age, and closer to the ages of broadly-equivalent eastern African australopiths than other southern African hominin age estimates (Section 2).

2 Wider context: conflicting chronologies for *Australopithecus*

Australopithecus in southern Africa is represented by at least two endemic species, *Australophithecus africanus* and *Australopithecus sediba*; the latter is known from palaeokarst locality Malapa, dated by U–Pb methods and magnetostratigraphy to 2.0 Ma (Pickering et al., 2011). *Australopithecus africanus* is known from four localities: Sterkfontein, Gladysvale, Makapansgat, and Taung.

Australopithecus africanus material has been retrieved from Sterkfontein Members 2 and 4; sediment from Member 2 has been dated to 3.67 ± 0.16 Ma (Granger et al., 2015) and from Member 4

to between 3.6 and 3.4 Ma (Granger et al., 2022) using cosmogenic $^{10}Be/^{26}Al$ burial dating. These dates conflict with flowstone U–Pb ages of ∼2.2 Ma from Member 2 (Walker et al., 2006; Pickering et al., 2019) and 2.8–2.0 Ma from Member 4 (Pickering and Kramers, 2010; Pickering et al., 2019); some explain this discrepancy by arguing that two-stage burial processes have produced excessively old cosmogenic ages (Kramers and Dirks, 2017); others have argued that the flowstones are stratigraphically 'intrusive', and post-date the hominin fossils (Bruxelles et al., 2019).

Australopithecus africanus from Gladysvale (Berger et al., 1993) is represented by two isolated teeth collected from an ex-situ lime dump and dated to approximately 2 Ma on the basis of biostratigraphic inference (Berger, 1993). Fossil hominins from Makapansgat, assigned by some to *Australopithecus africanus*, (Berger and Hawks, 2019) and others to *Australopithecus prometheus* (Clarke and Kuman, 2019) are dated to between 2.5–2.0 Ma using palaeomagnetic and biostratigraphic inferences. A recent study uses fossil cercopithecid biochronology (Frost et al., 2022) to suggest that there are no hominin sites in southern Africa older than ∼2.8 Ma. This implies that the Sterkfontein Member 2 and 4 cosmogenic isotope ages are incorrect, but does not explain why this might be. Unfortunately, all this means that presently no *Australopithecus africanus* fossils are associated with well-accepted and fully quantitative radiometric ages.

Despite the many chronological uncertainties associated with *Australopithecus* in southern Africa, it is often considered necessary to incorporate best-estimate chronological information (first and last appearance date; FAD and LAD) for *Australopithecus africanus* and *Australopithecus sediba* into hominin evolutionary analyses. Due to the above dating controversies, *Australopithecus africanus* is either given a maximum stratigraphic range (e.g. from 3.8 to 2.0 Ma) or a minimum stratigraphic range (e.g. 3.0 to 2.4 Ma); with many variations existing in the literature (e.g. Wood and K. Boyle, 2016; van Holstein and Foley, 2022, 2024; Püschel et al., 2021; Mongle et al., 2022). For *Australopithecus sediba*, with just one geological horizon available, the FAD and LAD are identical, and a number of statistical approaches are available to take this stratigraphic and sampling uncertainty into account (e.g. Hopley and Maxwell, 2022; van Holstein and Foley, 2024).

When the full age uncertainty is considered (3.8 to 2.0 Ma), *Australopithecus africanus* has the longest stratigraphic range of all fossil hominins, with the possible exception of *Homo erectus* (e.g. Wood and K. Boyle, 2016). This stratigraphic range exceeds that of the combined *Australopithecus anamensis* (4.2–3.9 Ma) and *Australopithecus afarensis* (3.7–3.0 Ma) anagenetic pairing, a far more abundant and well-dated collection of fossils. Either *Australopithecus africanus* was an unusually long-lived species, or poor dating accuracy and precision have resulted in an artificially expanded stratigraphic range.

With the exception of the single occurrence of the enigmatic *Australopithecus garhi* at 2.5 Ma (Asfaw et al., 1999) from the Bouri Formation of Ethiopia, the youngest occurrence of *Australopithecus* outside of South Africa is *Australopithecus afarensis* at 3.0 Ma from Hadar, Ethiopia (Alemseged et al., 2005). If the southern African australopiths are indeed younger than 3.0 Ma (as suggested by the most recent biostratigraphic inferences of Frost et al., 2022), then this represents a relict population following eastern African extirpation. An equally plausible scenario is that southern African and eastern African *Australopithecus* are broadly contemporaneous (from 4.0 to 3.0 Ma), as implied by the cosmogenic isotope ages of Granger et al. (2022), and that the current U–Pb and electron spin resonance (ESR) age estimates from southern Africa are too young (Figure 1a).

In a first attempt to reconcile the differences between the cosmogenic burial dates and the carbonate U–Pb dates, we re-calculated the latter from the raw isotopic ratio data reported in the

literature (see Section 4 for further details about these calculations). We managed to reproduce the dates but not their uncertainties. We found that the isochron dates reported in the literature do not take into account the excess scatter that characterises many of the U–Pb isochrons. The most extreme example of this is shown in Figure 1b for sample M6 of (Pickering et al., 2019). This sample is characterised by excess scatter 28 times the size of the analytical uncertainties. Inflating the uncertainty of the uncorrected U–Pb isochron age accordingly, removes the disagreement between the cosmogenic dates and the U–Pb dates for some samples, but not for all of them.

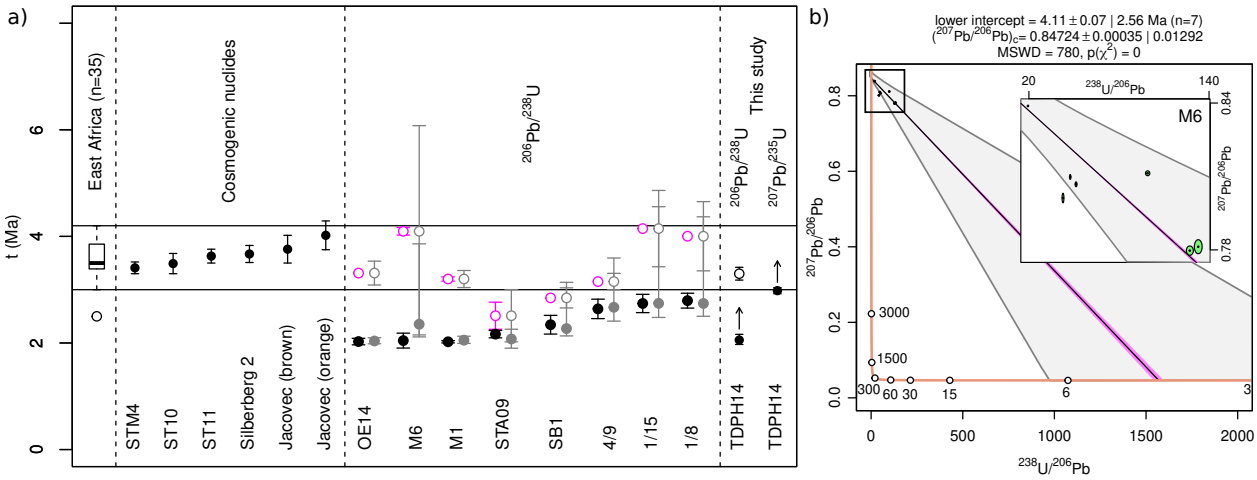

Figure 1: a) Compilation and comparison of *Australopithecus* chronologies for eastern Africa, shown as a box plot of hominin horizons (Maxwell et al., 2018) with *Australopithecus garhi* from the Bouri Formation in Ethiopia as a sole outlier; and southern Africa. Cosmogenic nuclide ages are as reported by Partridge et al. (2003) and Granger et al. (2015, 2022). $^{206}Pb/^{238}U$ ages (M6 and M1 from Malapa, the rest from Sterkfontein) are from Walker et al. (2006) and Pickering et al. (2019). STA09, SKA3 and SB1 are from the Silberberg Grotto and may not have a stratigraphic association with the Sterkfontein *Australopithecus* fossils (Bruxelles et al., 2019). Empty magenta and filled black plot symbols mark the U–Pb dates before and after disequilibrium correction, respectively, with uncertainties as reported in these publications. Grey symbols represent our attempt to recalculate these results from the original isotopic data (see panel b). Sample TDPH14 yields a new age estimate for the Taung skull, as discussed in Section 5. The arrows indicate that the $^{207}Pb/^{235}U$ isochron age and the disequilibrium-corrected $^{206}Pb/^{238}U$ isochron age are minimum estimates due to post-depositional U-uptake. Note that other southern African samples would be likely to show U mobility too, if $^{207}Pb/^{235}U$ data were available. b) Tera-Wasserburg diagram for sample M6, exhibiting extreme over-dispersion with respect to the analytical uncertainties. Expanding the uncertainty envelope (light grey) to account for this over-dispersion gives rise to the large grey error bars for the re-calculated U–Pb dates shown as empty grey symbols in panel a. The filled grey symbols and error bars of panel a represent the re-calculated disequilibrium corrections, ignoring overdispersion but assuming 2‰ reproducibility for the measured $^{234}U/^{238}U$ activity ratio measurements (Section 4.1).

3 Previous age estimates for Taung

3.1 Geological context

There are two faunal assemblages present within the Taung Type Site: the 'Dart Deposits' (D-A to D-E) exposed by excavations at the southern base of the Dart pinnacle (McKee, 2016) and the 'Hrdlička Deposits' (H-A to H-D) exposed on the top and southern face of the Hrdlička pinnacle (Hrdlčka, 1925; McKee and Tobias, 1994). Based on distinct vertebrate fossil assemblages and stratigraphic relationships, most studies recognise the two deposits as temporally distinct, with the Dart Deposits being older than the Hrdlička Deposits (McKee and Tobias, 1994; McKee, 2016; Frost et al., 2022). Furthermore, the Dart Deposits are consistently identified as the likely location of the Taung fossil (Tobias et al., 1993; McKee, 2016; Hopley and Kuhn, 2022). Most researchers, including Dart, have considered Taung to have been deposited within cave sediments formed within, or contemporaneously with, the Thabaseek tufa (e.g. Peabody, 1954; Tobias et al., 1993; McKee, 2016). However, recent reanalysis of the sedimentology and stratigraphy has indicated a more complex picture of palustrine and palaeosol environments within the Dart Deposits (Hopley et al., 2013; Kuhn et al., 2015; Parker et al., 2016) and the presence of cave/fissure sediments and speleothems in the Hrdlička Deposits (Hopley and Kuhn, 2022, see Environments Chapter). Due to the secondary nature of cave deposits, it is clear that the speleothems of the Hrdlička Deposits are the youngest sediments of the Taung Type Site and represent a minimum age constraint for the Taung fossil.

3.2 Biostratigraphy

Biostratigraphic age estimates rely on external independent sources of chronological information, ideally well-established radiometric ages. Prior to the first radiometric age estimates from the Cradle of Humankind (Partridge et al., 2003; Walker et al., 2006), biostratigraphic inferences relied upon faunal correlation with eastern African fossils assemblages associated with $^{40}Ar/^{39}Ar$ dated volcanic rocks. This approach was limited by the assumption that the FADs and LADs of species or genera are shared across distinct biogeographic regions, and because assigned ages are approximate and difficult to verify. Using this approach (McKee, 1993) gave the fauna from the Taung site a biostratigraphic age estimate of 2.8–2.6 Ma. After the publication of U–Pb flowstone ages from multiple southern African caves sites, Pickering et al. (2019) and Frost et al. (2022) were able to use radiometric ages from within the southern African faunal province to reduce the biogeographic uncertainties of their biostratigraphic inferences. The similarity of the cercopithecid faunas at Taung to those of Sterkfontein Members 2 and 4 led the authors to suggest an age of ∼2.8–2.0 Ma for Taung and ∼2.7–2.6 Ma for Makapansgat (Frost et al., 2022). The validity of this approach is dependent upon many factors, including the accuracy of the flowstone U–Pb ages from Sterkfontein, and as we explain below there are methodological reasons to question the accuracy of the U–Pb ages and the biostratigraphic inferences that depend on them. In the absence of radiometric age estimates, the age of the Taung fossil is typically reported as ∼2.8 Ma.

3.3 Radiometric geochronology

Vogel and Partridge (1984) obtained a $^{234}U/^{238}U$ disequilibrium date of 942 ± 90 ka for the top of the Thabaseek formation. A follow-up study by Tobias et al. (1993) produced two more dates of 999 ± 64 ka and 762 ± 13 ka, respectively. These dates are much younger than the biostratigraphic estimates and therefore influence the evolutionary significance of the Taung Child. A < 1 Ma

age would make Taung the youngest instead of one of the oldest specimen of *Australopithecus*, far younger than the hominins from Makapansgat, the Cradle of Humankind and eastern African australopiths.

One way to explain the young age estimates is that Taung belongs to a relict population of hominins who survived on the edge of the Kalahari desert when *Australopithecus* was already extinct elsewhere on the African continent (Tobias, 1973; Tobias et al., 1993; McKee, 1993). However, the truth is likely to be more mundaine. The Th/U disequilibrium dates are probably wrong or, more precisely, they do not record the formation age of the Thabaseek tufa. The very high $^{234}U/^{238}U$-activity ratios measured by Vogel and Partridge (1984), and the unusual variability of the dates presented by Tobias et al. (1993) likely reflect open system behaviour, whereby uranium was added or substituted after deposition (Tobias et al., 1993). There have been no subsequent attempts to produce radiometric ages for the Taung Type Site, instead researchers have had to settle for biostratigraphic inference.

4 Introduction to carbonate U–Pb geochronology

The U–Pb method is one of the most versatile and powerful techniques in the geochronological toolbox. It is presently most commonly used to date accessory minerals such as zircon, but it is increasingly applied to other materials as well, including carbonates. The U–Pb method is appealing in several ways. First, it does not have an upper age limit. Whereas the Th/U disequilibrium method works best for samples of < 500 ka, the U–Pb method works best for samples of > 500 ka. In this sense, the U–Pb method is complementary to Th/U disequilibrium dating.

Second, the U–Pb method contains an internal quality control mechanism of sorts, something that is absent from most other geochronometers. This mechanism is based on the fact that natural uranium contains two long lived isotopes (^{238}U and ^{235}U), which decay to two different lead isotopes (^{206}Pb and ^{207}Pb, respectively). These two decay mechanisms produce two age estimates. If the $^{206}Pb/^{238}U$- and $^{207}Pb/^{235}U$-dates agree, then this gives the analyst greater confidence the results are accurate.

Carbonate U–Pb dating is not easy. In contrast with zircon, which incorporates relatively high U-concentrations and low Pb-concentrations in its crystal lattice, carbonate minerals (calcite, dolomite, aragonite) tend to be poor in U and comparatively rich in Pb. This 'parentless' or 'common' Pb has to be quantified in order to determine the residual 'radiogenic' Pb that decayed from its uranium parent isotope, and this introduces additional uncertainty.

The common Pb problem can be solved by analysing multiple cogenetic aliquots of the same sample, and normalising the U- and Pb-measurements to a non-radiogenic lead isotope, ^{204}Pb. This gives rise to two coupled 'isochron' equations:

$$\begin{cases} \frac{^{206}Pb}{^{204}Pb} = \left[\frac{^{206}Pb}{^{204}Pb}\right]_0 + \left[\frac{^{238}U}{^{204}Pb}\right](\exp[\lambda_{238}t] - 1) \\ \frac{^{207}Pb}{^{204}Pb} = \left[\frac{^{207}Pb}{^{204}Pb}\right]_0 + \left[\frac{^{235}U}{^{204}Pb}\right](\exp[\lambda_{235}t] - 1) \end{cases} \quad (1)$$

where λ_{238} and λ_{235} are the decay constants of ^{238}U and ^{235}U, respectively; and t is the age of the sample. Equation 1 forms two straight lines whose intercepts correspond to the common-Pb ratios ($[^{206}Pb/^{204}Pb]_0$ and $[^{207}Pb/^{204}Pb]_0$, respectively). In the case of many carbonate samples, ^{208}Pb can be used instead of ^{204}Pb (Parrish et al., 2018). This substitution is possible because the

radioactive parent of ^{208}Pb is ^{232}Th, which is not generally soluble in water and therefore of very low general abundance relative to U in carbonate.

^{208}Pb offers two advantages over ^{204}Pb. First, it is > 30 times more abundant, making it easier to measure and requiring shorter mass spectrometer dwell times, thereby improving analytical precision. Second, ^{208}Pb is unaffected by an isobaric interference of ^{204}Hg, which makes ^{204}Pb difficult to measure by ICP-MS.

For datasets in which neither ^{204}Pb nor ^{208}Pb are available, common Pb correction can also be done by plotting the ^{207}Pb/^{206}Pb-ratio against the ^{238}U/^{206}Pb-ratio (a 'Tera-Wasserburg' diagram, Figure 1.b) and constructing a 'semitotal-Pb/U isochron' (Ludwig, 1998). The main limitation of this simpler approach is that it assumes concordance of the ^{207}Pb/^{235}U and ^{206}Pb/^{238}U clocks. Because the Tera-Wasserburg diagram relies on ^{206}Pb and ^{207}Pb for both deconvoluting common and radiogenic Pb, it is less able to resolve Pb loss from common Pb heterogeneity.

4.1 Initial disequilibrium corrections

Although Equation 1 represents two ways to date carbonate rocks, in practice the ^{206}Pb/^{238}U-clock is given far more weight than the ^{207}Pb/^{235}U-clock. This is because ^{238}U is $\sim$138 times more abundant than ^{235}U. Consequently, ^{206}Pb is more abundant* and, hence, easier to measure than ^{207}Pb. The main limitation of the ^{206}Pb/^{238}U method – and the Achilles heel of carbonate U–Pb geochronology – is the assumption of initial secular equilibrium that underlies Equation 1. The problem is that ^{238}U does not decay directly to ^{206}Pb, but passes by 13 short-lived intermediate daughter 'stations'. The longest-lived of these intermediate daughters are ^{234}U ($t_{1/2} = 245$ kyr) and ^{230}Th ($t_{1/2} = 75$ kyr). Any initial excess or deficit of these intermediate daughters results in an over- or under-estimated date, respectively. Removing the resulting biases requires a correction for any initial disequilibrium.

In the case of ^{230}Th, this correction is easy. As mentioned before, Th is insoluble in water and is therefore generally negligible from newly formed carbonate. It is safe to assume that these conditions also apply to the initial concentrations of ancient carbonates, and a simple mathematical correction can be applied. Unfortunately, the case of ^{234}U is not so straightforward. Unlike ^{230}Th, which always starts off with a deficit relative to ^{238}U, ^{234}U can either exhibit an initial deficit or, more commonly, an initial excess relative to ^{238}U.

In some karst settings in southern Africa, the excess can reach values up to a factor of 12 and be highly variable through time (Kronfeld et al., 1994). In fact, in Section 3.3 we have already shown how parts of the Thabaseek formation are characterised by strong ^{234}U/^{238}U-fractionations, which cannot safely be assumed to remain constant through time. Applying an initial ^{234}U-correction based on an a priori estimate partly defeats the purpose of the U–Pb method, reducing its key advantage over Th/U disequilibrium dating. Correcting U–Pb dates for initial ^{234}U/^{238}U disequilibrium requires accurate estimates of the initial ^{234}U/^{238}U activity ratio. The only way to obtain such estimates without making unverifiable assumptions is to measure any remaining ^{234}U/^{238}U disequilibrium and inferring the initial value iteratively on the assumption of a closed system.

Accurate disequilibrium corrections are only possible for relatively young samples. Beyond ~ 2 Ma, even the most extreme initial ^{234}U/^{238}U activity ratios have decayed back to a state that is impossible to distinguish from secular equilibrium. For example, after 2 Ma, an initial ^{234}U/^{238}U activity ratio of 3 will be reduced to a value of 1.001782, which is only 1.7 ‰ above the equilibrium

*^{206}Pb is not 138 but < 23 times more abundant than ^{207}Pb due to the shorter half-life of ^{235}U compared to ^{238}U.

ratio of 1.000055 ($\equiv \lambda_{234}/[\lambda_{234} - \lambda_{238}]$, McLean et al., 2016). Even if an analytical precision of 1 ‰ is possible, this uncertainty balloons when extrapolating to estimate the initial ratio.

In reality, the situation is even worse because the analytical precision of $^{234}U/^{238}U$ measurements tends to underestimate the dispersion observed when analysing duplicate samples. For example, Walker et al. (2006) carried out ten replicate $^{234}U/^{238}U$ analyses on different aliquots of a Sterkfontein speleothem (Figure 2). With an MSWD of 2.4 and a $p(\chi^2)$ value of 0.01, the weighted mean of these measurements is over-dispersed by about 20% with respect to the analytical uncertainties. This overdispersion corresponds to an irreducible uncertainty of ~ 2‰ for the $^{234}U/^{238}U$ activity ratio. The precision on a single analysis of $^{234}U/^{238}U$ for a locale or specimen would risk false confidence that the measurement was accurate and/or precise, and could lead to the illusion that the final age is robust.

The possible bias caused by inaccurate disequilibrium corrections can be substantial. Beyond 1.5 Ma, the uncertainty of the disequilibrium may exceed the correction itself. As a consequence, carbonate U–Pb dating is subject to the same maximum age limits as Th/U disequilibrium dating.

4.2 A critical appraisal of existing U–Pb dates for southern African hominin sites

Figure 3 presents a selection of 31 published carbonate U–Pb data from southern African hominin discovery sites, including the landmark study of Walker et al. (2006), the Malapa data of Dirks et al. (2010) and the 26-sample compilation of Pickering et al. (2019). The new Taung data from Section 5 are also shown for comparison.

The figure consists of two parts. Panel a) shows the magnitude of the disequilibrium correction. Panel b) shows its precision. Solid lines represent different initial $^{234}U/^{238}U$-activity ratios. The initial $^{230}Th/^{238}U$-activity ratio was assumed to be zero ($[^{230}Th/^{238}U]_i = 0$) in all cases.

The magnitude of the disequilibrium correction (panel a) was calculated as follows:

1. Given the initial $^{234}U/^{238}U$-activity ratio and the disequilibrium-corrected U–Pb age (t_c), predict the present-day $^{206}Pb/^{238}U$-ratio.
2. Use this $^{206}Pb/^{238}U$-ratio to calculate the uncorrected ('raw') $^{206}Pb/^{238}U$-date (t_r).
3. Define the relative magnitude of the disequilibrium correction as $(t_r - t_c)/t_c$. Note that this is an 'optimistic' way to quantify the size of the correction. Using the corrected age in the numerator would produce larger values.

Panel a) relates to the accuracy of the disequilibrium correction: the greater the correction, the more likely it is to be inaccurate. In contrast, panel b) visualises the precision of the correction. This is calculated as follows:

1. Use the initial $^{234}U/^{238}U$-activity ratio ($[^{234}U/^{238}U]_i$) to predict the present-day $^{234}U/^{238}U$-activity ratio ($[^{234}U/^{238}U]_m$) and the present-day $^{206}Pb/^{238}U$ ratio.
2. Add/subtract 2‰ uncertainty to/from $[^{234}U/^{238}U]_m$ to obtain two limits $[^{234}U/^{238}U]_u$ and $[^{234}U/^{238}U]_l$, respectively. Note that this calculation ignores the overdispersion issues highlighted in Figure 1 and, therefore, paints an optimistic picture of the situation.

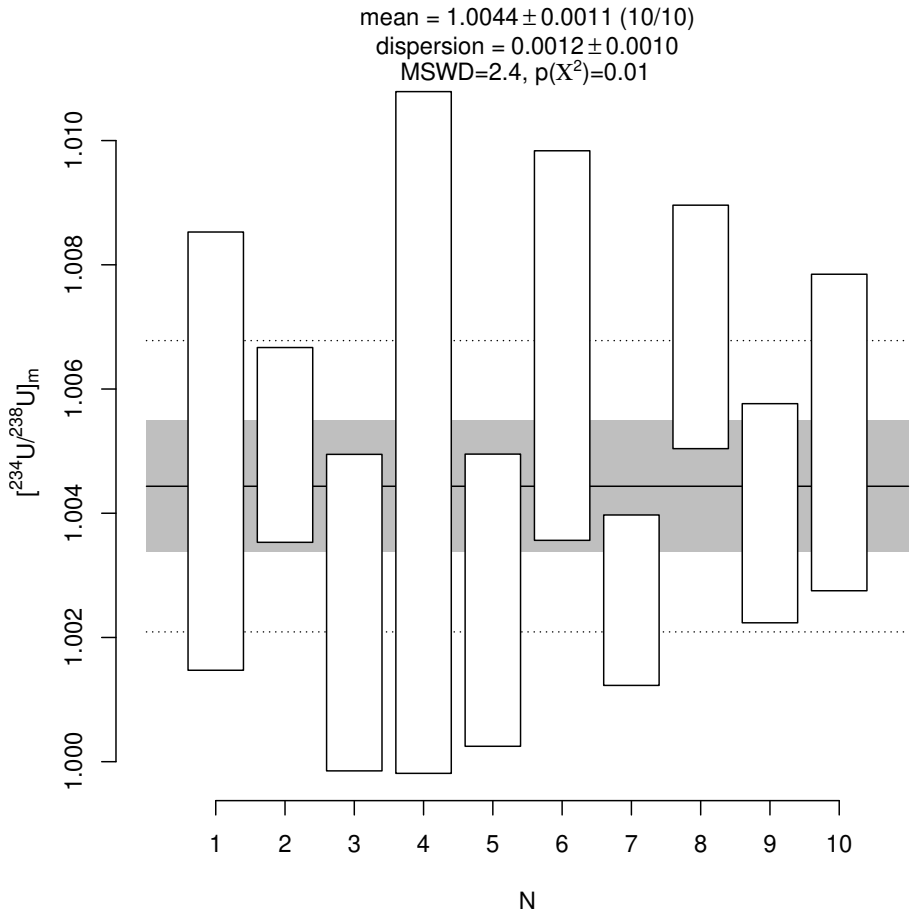

Figure 2: Ten replicate $[^{234}U/^{238}U]$-activity ratio measurements from Walker et al. (2006). The grey band marks the 95% confidence interval for the weighted mean. The high MSWD and low p-value indicate that the dataset is overdispersed with respect to the analytical uncertainties. The overdispersion can be described by a random effects model with two sources of variance corresponding to the analytical uncertainty and the 'dispersion', respectively (Vermeesch et al., 2012). The dotted line marks the 95% confidence interval corresponding to the dispersion. For the Walker et al. (2006) dataset, it is about 2‰ wide.

3. Combine $[^{234}U/^{238}U]_u$ and $[^{234}U/^{238}U]_l$ with the predicted $^{206}Pb/^{238}U$-ratio from step 1 to obtain two age limits t_l and t_u.

4. Define the relative precision as $(t_u - t_l)/t_c$.

The solid lines of Figure 3b terminate where it is no longer possible to obtain a physically-plausible solution. This can either happen when $[^{234}U/^{238}U]_l < 1.000055$ and t is sufficiently high so that $[^{234}U/^{238}U]_i = 0$; or when $[^{234}U/^{238}U]_l > 1.000055$ and t is sufficiently high so that $[^{234}U/^{238}U]_i > 20$.

The dashed line in Figure 3.b marks the uncertainty envelope for $^{206}Pb/^{238}U$ dates that lack initial disequilibrium constraints, either because $^{206}Pb/^{238}U$ was not measured or because the disequilibrium has expired. This envelope was calculated as the difference between the $^{206}Pb/^{238}U$-date with an initial $^{234}U/^{238}U$-activity ratio $[^{234}U/^{238}U]_i = 12$ (the highest value reported by Kronfeld et al., 1994) and $[^{206}Pb/^{238}U]_i = 1$ (no initial uranium disequilibrium).

In absolute terms, Δt increases from 0 Myr at $t = 0$ to 3.9 Myr at $t = \infty$, but in relative terms, the uncertainty decreases from $\Delta t/t = \infty$ at $t = 0$ to $\Delta t/t = 0$ at $t = \infty$. At the 2–4 Ma timescales of interest, the unconstrained $^{206}Pb/^{238}U$ age uncertainty hovers around 80–90%. This large uncertainty is the reason why it is so important to apply a disequilibrium correction to carbonate $^{206}Pb/^{238}U$-dates in the first place, particularly in areas of high $[^{234}U/^{238}U]_i$ variability such as the Cradle of Humankind.

For sufficiently old samples, the uncertainty of the disequilibrium correction (i.e., $t_u - t_l$) may exceed the correction itself ($t_r - t_c$). For initial $^{234}U/^{238}U$ activity ratios of 1, 2 and 4 (assuming $[^{230}Th/^{238}U]_i = 0$), this occurs for ages exceeding 1.54, 2.04 and 2.58 Ma, respectively.

Thirty-two U–Pb measurements are shown as circles in Figure 3. Half of them are associated with disequilibrium corrections exceeding 30% of the uncorrected age (corresponding to 43% of the corrected age), and uncertainties of greater than 10%. Four samples fall in the 'forbidden zone' with unresolvable $[^{234}U/^{238}U]_i$-values. It is also useful to observe that the oldest samples tend to have the highest inferred $[^{234}U/^{238}U]_i$-values. This is likely a numerical artifact caused by extrapolation of a very small amount of residual disequilibrium and/or open system behaviour with addition or replacement of initial U with U with more marked disequilibrium.

In summary, Figure 3 casts doubt on the value of disequilibrium-corrected carbonate $^{206}Pb/^{238}U$ dates. Fortunately, there is a solution to the $^{234}U/^{238}U$ disequilibrium conundrum. For old samples, the complications of the $^{234}U/^{238}U$ disequilibrium correction can be circumvented by avoiding the $^{206}Pb/^{238}U$-method altogether, and using the $^{207}U/^{235}U$-method instead. This will be explained in the next section.

4.3 The $^{207}Pb/^{235}U$ method

Even though the $^{207}Pb/^{235}U$ clock is less precise than the (uncorrected) $^{206}Pb/^{238}U$ clock, it can be precise enough for samples that are reasonably old and relatively rich in uranium. Crucially, the loss of precision is compensated by a gain in accuracy (Richards et al., 1998; Vaks et al., 2020; Engel et al., 2019).

Whereas the ^{238}U decay series contains two long-lived intermediate daughters, the ^{235}U series contains only one such daughter, ^{231}Pa ($t_{1/2} = 32.7$ kyr). This nuclide is easy to deal with because Pa is chemically similar to Th. Therefore, ^{231}Pa is always depleted in newly formed carbonates, so that its initial activity ratio can be safely neglected. Even if the assumption of zero ^{231}Pa is wrong, the consequences of this wrong assumption are small. This is because, unlike the ^{234}U correction, which can range from -17% to $> +100\%$, the ^{231}Pa correction only ranges from -2% to 0% (assuming a true age of 2 Ma). There are two reasons why the southern African carbonate U–Pb datasets of Pickering et al. (2019), Dirks et al. (2010) and Walker et al. (2006) cannot be re-evaluated using the $^{207}Pb/^{235}U$ method.

First, the data tables provided in these publications are formatted in terms of $^{238}U/^{206}Pb$, $^{207}Pb/^{206}Pb$ and $^{204}Pb/^{206}Pb$ ratios. In principle, it is possible to compute the $^{207}Pb/^{235}U$ ratio from the $^{238}U/^{206}Pb$ and $^{207}Pb/^{206}Pb$ ratios, provided that the error correlation between all the

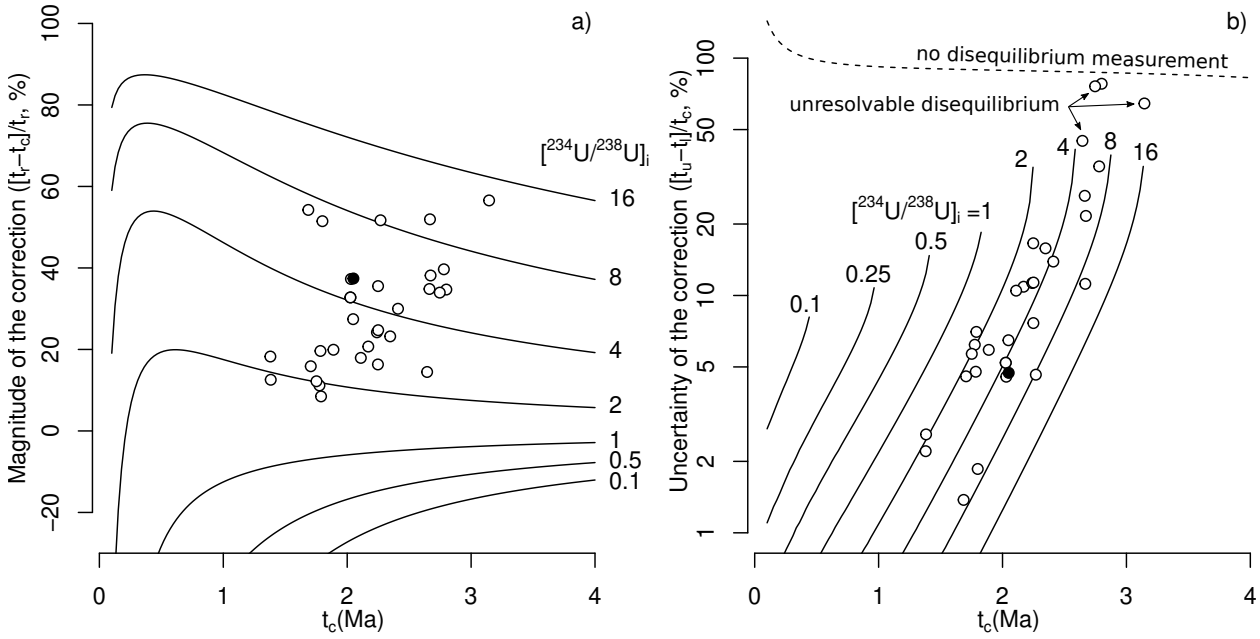

Figure 3: Relative magnitude (a) and precision (b) of the initial $^{234}U/^{238}U$ disequilibrium correction against the corrected carbonate $^{206}Pb/^{238}U$ date (t_c), for different values of the initial $^{234}U/^{238}U$ activity ratio (solid lines). The dashed line in panel b) marks the relative uncertainty interval when no disequilibrium measurement is available, defined as the difference between corrected dates using assumed initial $^{234}U/^{238}U$ activity ratios of 1 and 12. Empty circles mark 31 published U–Pb dates from Walker et al. (2006), Dirks et al. (2010) and Pickering et al. (2019) listed in Table 1. The black circles mark the new U–Pb date for Taung sample TDPH14 (Section 5). Panel a) shows that this sample has a disequilibrium-corrected U-Pb date (t_c) of 2.05 Ma, which is 40% younger than the uncorrected date (t_r). This age difference is caused by an iteratively calculated initial $^{234}U/^{238}U$-activity ratio of 4.9. Assuming a reproducibility of the present-day $^{234}U/^{238}U$ measurement of 2‰, panel b) shows that the disequilibrium correction has an analytical precision of 5%. The four published datasets marked by the arrows in panel b) have measured $^{234}U/^{238}U$ activity ratios that are within 2‰ of secular equilibrium.

ratios are provided. Unfortunately, most of these error correlations are either not provided with the published southern African flowstone U–Pb datasets, or they are suspect due to the presence of physically impossible values (< -1 or > 1). This is why Figure 1.b assumes zero error correlations (error ellipses parellel to the plot axes).

Second, many of these published studies do not provide information on ^{208}Pb. This is unfortunate because ^{208}Pb can be measured more precisely than ^{204}Pb, which is important to compensate for the lower precision of the $^{207}Pb/^{235}U$ ratio measurements. Fortunately, some studies do include ^{208}Pb ratios, including those of Walker (2005) and Walker et al. (2006). Figure 4 shows an unpublished ID-TIMS dataset from a lone sample (LAB03) of the Makapansgat Limeworks presented by Walker (2005). Neither the dataset of Walker (2005) nor that of Walker et al. (2006) provides all the error correlations needed to fully propagate the uncertainties of the isochron ratios.

The LAB03 sample is a piece of Member 1b flowstone collected from the area between the Original Ancient Entrance (OAE) and the North Alcove of the Main Quarry (Walker, 2005; Reed

et al., 2022). The flowstone was deposited prior to the in-filling of the cave with clastic sediments, so is older than all the fossil-bearing units of the Makapansgat Limeworks: Members 2–5 and Rodent Corner (Maguire, 1984; Reed et al., 2022). Unfortunately, it is not currently possible to determine the time that elapsed between the deposition of Member 1b flowstone and the overlying sedimentary units. Most of the *Australopithecus* fossils were collected *ex situ* from lime dumps and have been confidently assigned to Member 3; therefore, LAB03 provides a maximum age estimate for all fossils including *Australopithecus africanus* from the Makapansgat Limeworks.

With this caveat in mind, Figure 4 conveys several important pieces of information. First, the LAB03 sample is old (> 4.4 Ma using the 95% confidence interval for the $^{207}Pb/^{235}U$ isochron age as a lower bound). This antiquity is consistent with biostratigraphic evidence for Makapansgat Member 3 being among the oldest fossil assemblages in southern Africa (McKee, 1993; Frost et al., 2022) and with magnetostratigraphic inference for the OAE flowstones belonging to the Gilbert magnetochron at approximately 4 Ma (Hopley et al., 2007). The age of LAB03 is also comparable with the 4.9 ± 1.9 Ma $^{207}Pb/^{235}U$ isochron age for the Hoogland Basal Speleothem (Hopley et al., 2019), suggesting that Mio-Pliocene age flowstones may be a common feature of southern African palaeo-karst. Second, there is a significant difference between the $^{206}Pb/^{238}U$ and $^{207}Pb/^{235}U$ isochron ages (7.92 and 5.28 Ma, respectively). Third, the $^{207}Pb/^{235}U$ date is less precise than the $^{206}Pb/^{238}U$ date, with 95% confidence intervals of 0.11 and 0.87 Ma wide, respectively.

The significant difference between the two types of U–Pb dates for LAB03 is likely the result of initial $^{234}U/^{238}U$ disequilibrium. Due to its old age, it is not possible to undo the effects of this disequilibrium. However, we do know that the effect of $^{234}U/^{238}U$ disequilibrium on $^{206}Pb/^{238}U$ isochrons can exceed 1 Ma, whereas the effect of $^{231}Pa/^{235}U$ disequilibrium is capped at 30 ka (Section 4.3). Therefore, we conclude that the $^{207}Pb/^{235}U$ isochron is more accurate than the $^{206}Pb/^{238}U$ isochron, amply compensating for its lesser precision.

Having illustrated the $^{207}Pb/^{235}U$ method, we reiterate that the results shown in Figure 4 are negatively affected by the absence of a full covariance structure. Knowledge of all error correlations would improve the precision of the estimated isochron age. In order to take full advantage of the $^{207}Pb/^{235}U$ method, it is necessary to either reprocess the raw mass spectrometer data from the published studies that report ^{204}Pb and/or ^{208}Pb, or to start over again and re-analyse all the hominin discovery sites. The next section will start this effort with some new $^{207}Pb/^{235}U$ dates, which we believe to serve as a robust minimum age constraint for Taung.

5 New U–Pb age constraints for Taung

During the 2010 field season at the Taung site, a number of carbonate samples (speleothems and tufas) were collected from the Dart pinnacle, the Hrdlička pinnacle, and the intervening deposits exposed in the quarry floor of the disused Buxton-Norlim limeworks. The samples were screened by LA-ICP-MS to assess their suitability for U–Pb dating. Suitable samples exhibit relatively high U-concentrations and a wide range of Pb/U-ratios providing the potential to form a well defined isochron line. Only one sample fulfilled all these criteria.

TDPH14 is a flowstone that was collected near the top of the Hrdlička pinnacle at an altitude of 1150 m a.s.l. (see Figure 5.i and the Environments Chapter for further details). The sample is a steeply-dipping brown and white flowstone, approximately 10 cm thick and composed of both aragonite and calcite. Its position high in the stratigraphic sequence, and its cavity-filling nature, offer a minimum age for both the Taung Type Site and the Taung skull.

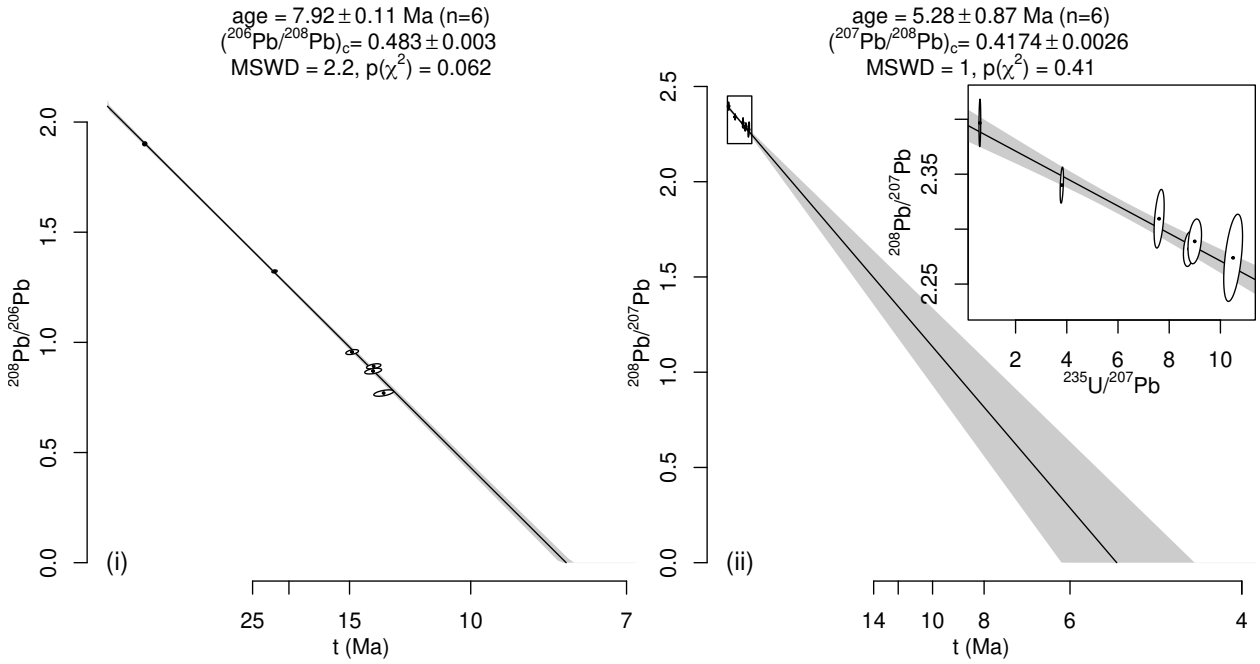

Figure 4: TIMS U–Pb data for Makapansgat Limeworks sample LAB03 of Walker (2005), presented as (i) $^{206}Pb/^{238}U$ and (ii) $^{207}Pb/^{235}U$ inverse isochrons (Li and Vermeesch, 2021). The former is more precise but less accurate than the latter, due to the inability to correct for initial disequilibrium beyond 2 Ma. Error correlations for these inverse isochron plots were calculated from the conventional isochron ratios reported in the data source, which were assumed to be uncorrelated. This assumption is likely incorrect, which has a minor effect on the isochron age and a major effect on its uncertainty, which is therefore wrong. Note that knowledge of the error correlations would reduce the uncertainty of the fit.

The sample was cut, polished and subjected to a preliminary isotopic analysis along an LA-ICP-MS transect (Figure 5.ii). This screening revealed significant variability in U-concentration across the flowstone's laminations, with values ranging from 1 ppb to 35 ppm (Figure 5.iii). Targeting the most radiogenic layers of the sample yields a $^{206}Pb/^{238}U$ date of 3.166 ± 0.065 Ma (Figure 5.v). This falls well outside the detectable range for $^{234}U/^{238}U$ disequilibrium, casting doubt on the accuracy of the LA-ICP-MS data. Unfortunately, ^{207}Pb and ^{208}Pb signals were too low to construct a sufficiently precise $^{207}Pb/^{235}U$ isochron. A more precise ID-TIMS analysis of four aliquots of TDPH was undertaken to remediate this issue.

Four aliquots of TDPH14 yield an uncorrected $^{206}Pb/^{238}U$ 'errorchron' age of 3.30 ± 0.12 Ma (MSWD=49), which agrees with the LA-ICP-MS age (Figure 6.ii). Isotope dilution ICP-MS analysis of the sample indicates a present-day $^{234}U/^{238}U$ activity ratio of 1.0117 ± 0.0059 (Figure 6.iii). The $^{234}U/^{238}U$ activity ratio measurements are over-dispersed with respect to the analytical uncertainties. Due to the small number of aliquots (i.e., four), it is not possible to identify 'outliers' or to quantify the over-dispersion. Taking the weighted mean $^{234}U/^{238}U$ ratio at face value and using it to correct the $^{206}Pb/^{238}U$ isochron for initial disequilibrium changes the date from 3.30 ± 0.12 to $2.05 + 0.11/-0.08$ Ma. This 40% reduction in age implies an initial $^{234}U/^{238}U$ activity ratio of 4.9 (Figure 6.iv).

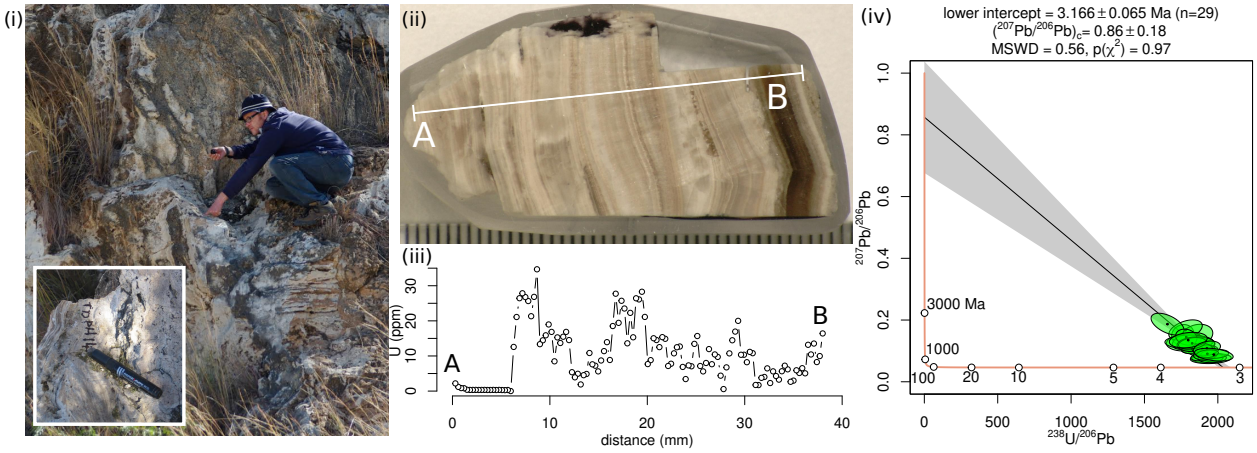

Figure 5: LA-ICP-MS data for sample TDPH14. (i) Field photograph of the sample location; (ii) a polished hand specimen of the sample; (iii) uranium concentration along the profile shown in the previous panel; (iv) semitotal-Pb/U isochron from a targeted high-U zone. The ^{238}U–^{206}Pb ratios are not corrected for initial disequilibrium.

Switching to ^{207}Pb/^{235}U space yields a well defined isochron of 2.982 ± 0.057 Ma (assuming no initial ^{231}Pa). This is similar to the uncorrected ^{206}Pb/^{238}U isochron age, implying that the sample was close to secular ^{234}U/^{238}U equilibrium at the time of formation. The ^{207}Pb/^{235}U isochron is more precise than the disequilibrium-corrected ^{206}Pb/^{238}U isochron. It is also less dispersed with an MSWD of 0.7 as opposed to value of 49 for the ^{206}Pb/^{238}U isochron. The two isochron age estimates do not overlap within the analytical uncertainties. This disagreement may be caused by open system behaviour of uranium, similar to that which was reported by Tobias et al. (1993) for the Th/U data of Vogel and Partridge (1984) and Tobias et al. (1993). Recent changes in ^{234}U/^{238}U activity ratios would result in an over-estimated ^{234}U/^{238}U-disequilibrium correction and, hence, an under-estimated ^{206}Pb/^{238}U isochron age. It would have a similar but smaller effect on the ^{207}Pb/^{235}U age. It is possible that the lower MSWD of the ^{207}Pb/^{235}U isochron reflects the smaller degree of isotopic disturbance.

Assuming uranium is only gained and not lost over time, both the disequilibrium-corrected ^{206}Pb/^{238}U and ^{207}Pb/^{235}U isochron ages are minimum age estimates. Consequently, the oldest date is the most useful one. Hence, we use the ^{207}Pb/^{235}U age to constrain the age of TDPH14. Given its location at the top of the Hrdlička pinnacle, and following Hopley et al. (2013)'s interpretation that the hominin-bearing unit was laid down in stratigraphic succession with the surrounding tufa deposits, the new flowstone date provides a lower age limit for the Taung skull. In order to obtain a potential upper age bracket for the fossil, a second sample is needed from below the PCS horizon. To this end, two boreholes were drilled in 2012 (see Environments Chapter), one in the Dart pinnacle (13.7 m) and one in the Hrdlička pinnacle (48.5 m). Unfortunately, LA-ICP-MS screening of neither core yielded any suitable material for U–Pb dating. The search for an upper age limit continues.

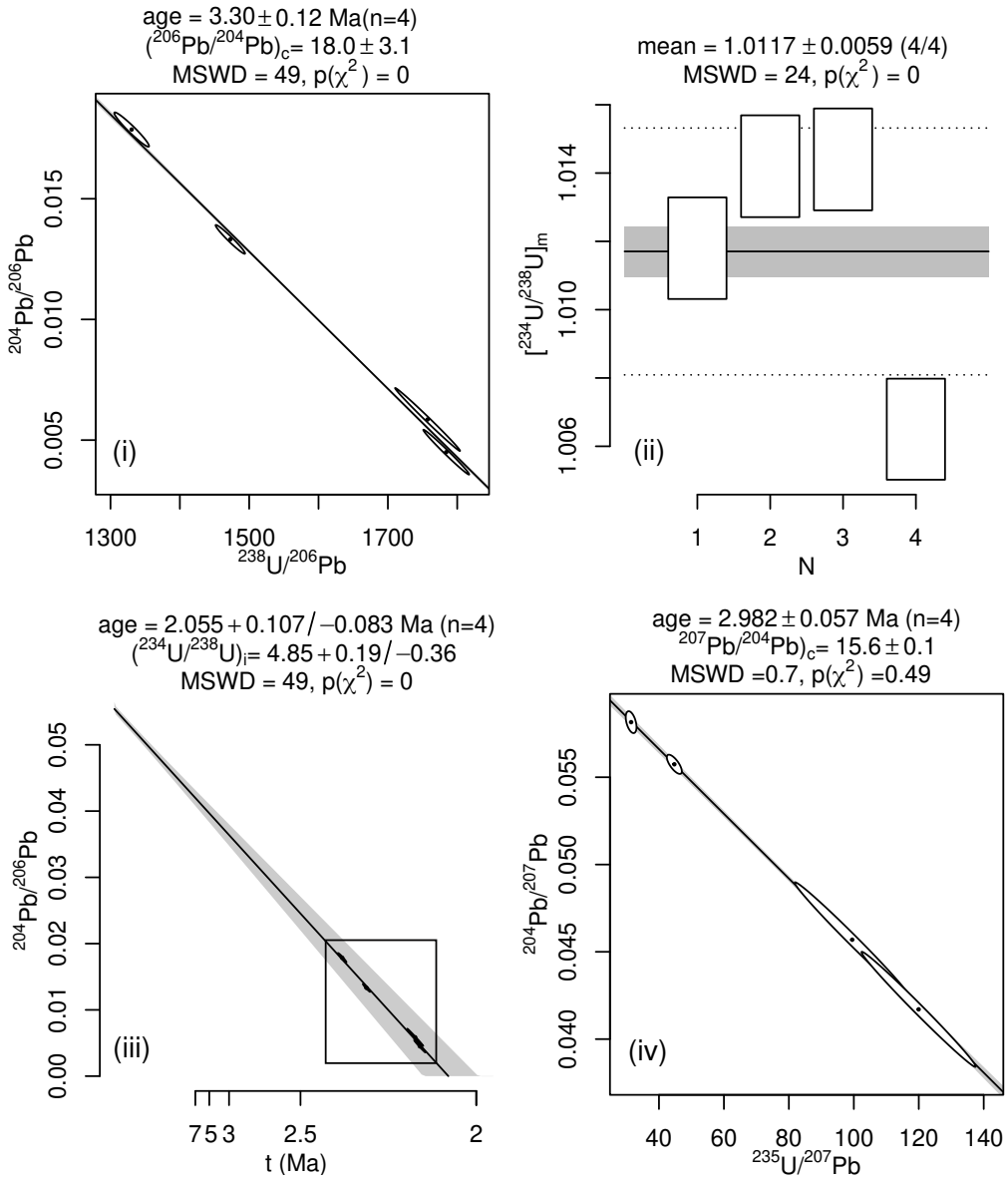

Figure 6: TIMS U–Pb data for sample TDPH14, shown as inverse isochrons. (i) uncorrected ^{238}U–^{206}Pb isochron; (ii) measured ^{234}U/^{238}U-activity ratios; (iii) disequilibrium-corrected ^{238}U–^{206}Pb isochron with a box showing the outline of panel i; (iiv) ^{235}U–^{207}Pb isochron. Data are reported in Table 2.

6 Conclusion

Since its discovery a century ago, Taung has challenged scientists. With the fossil itself being just a partially preserved juvenile skull, it took nearly two decades before most palaeoanthropologists agreed it was a human ancestor (Keith, 1947). This helped settle the debate between proponents of Asia and Africa being the origin of the hominin clade.

The age of Taung, and of other early southern African hominins, remains poorly constrained,

and this contribution has summarised just a subset of the numerous attempts to resolve this issue. In addition to the biostratigraphic and isotopic methods discussed above, archaeologists have applied numerous other dating techniques to the southern African hominin sites, including electron spin resonance dating, palaeomagnetic surveys, optically and thermally stimulated luminescence dating, and even U–Th–He thermochronology (Schwarcz et al., 1994; Herries and Shaw, 2011; Pickering et al., 2013; Makhubela and Kramers, 2022).

With so many inconsistent dates to choose from, there is a risk that palaeoanthropologists will pick the dates that best suit their preconceived ideas about human evolution. This potentially leads to circular reasoning and impedes scientific progress. Better and more consistent absolute dating methods are needed to break out of this cycle. The challenges posed by the southern African australopiths in general, and by Taung in particular, are an important driving force for methodological developments in radiometic geochronology.

The advent, nearly 20 years ago, of carbonate U–Pb geochronology, promised to be the much sought after breakthrough (Walker et al., 2006). Disequilibrium-corrected $^{206}Pb/^{238}U$ isochron dates were subsequently determined on dozens of southern African flowstones, most of which are summarised in Figure 3. The results of these studies suggest that the southern African hominins were substantially younger than their eastern African counterparts, and some researchers have drawn detailed environmental conclusions from these dates (Pickering et al., 2019). However, given the importance of the research questions at hand, it is important to remain vigilant and self-critical.

The disagreement between the U–Pb dates and independently-determined cosmogenic nuclide dates at Sterkfontein raises questions about the geological significance of these results (Granger et al., 2015; Kramers and Dirks, 2017; Granger et al., 2022). The quantitative analysis presented in this contribution reveals that the analytical uncertainty of several disequilibrium-corrected $^{206}Pb/^{238}U$ isochron dates has been under-estimated by hundreds of thousands of years, and in some cases more than a million years.

We advocate the use of the $^{207}Pb/^{235}U$ isochron method as a more accurate alternative. Our proposal simplifies a suggestion by Engel et al. (2019), who point out that the $^{207}Pb/^{235}U$ age should be concordant with the $^{206}Pb/^{238}U$ age, and that this concordance could be used to back-calculate the initial $^{234}U/^{238}U$ ratio in cases where reliable $^{234}U/^{238}U$ measurements are not possible. Engel et al. (2019) suggest using this inferred activity ratio to obtain a disequilibrium-corrected $^{206}Pb/^{238}U$ date. We argue that if the $^{207}Pb/^{235}U$ and $^{206}Pb/^{238}U$ ages are incompatible, then the $^{207}Pb/^{235}U$ age is far more likely to be correct, and should be taken as the best estimate of the true age. Beyond 2 Ma (and, in some cases, before that), all the age-resolving power of the paired $^{206}Pb/^{238}U$ and $^{207}Pb/^{235}U$ approach resides in the $^{207}Pb/^{235}U$ clock, so the $^{206}Pb/^{238}U$ data add no value.

Although we did not manage to obtain a definitive age estimate for the Taung skull in time for the centenary celebration of its discovery, we did make some meaningful progress towards this goal. We used the $^{207}Pb/^{235}U$ method to provide a tentative ~ 5.28 Ma upper age limit for the Makapansgat Limeworks deposit, which has been biostratigraphically linked to Taung (McKee, 1993). We also obtained a minimum age estimate of 2.98 ± 0.06 Ma for the Taung skull.

These preliminary results open the prospect of future progress. Our $^{207}Pb/^{235}U$ isochron age is closer to the uncorrected $^{206}Pb/^{238}U$ age than it is to the disequilibrium-corrected $^{206}Pb/^{238}U$ age. Naively assuming that the same phenomenon applies to other hominin discovery sites would resolve the discrepancy between the cosmogenic nuclide and U–Pb dates shown in Figure 1.

It would be premature to claim success. A lot more work is needed and it is unlikely that the

$^{207}Pb/^{235}U$ method is the panacea for all of the problems linked to dating the southern African australopiths. One issue is that post-depositional uranium uptake remains a challenge. Although the $^{207}Pb/^{235}U$ method is less affected by it than the $^{206}Pb/^{238}U$ and Th/U methods, it is not immune.

The debate about the relevance of the Taung skull was concluded when once vocal opponents of Raymond Dart's hypothesis graciously admitted that they had been wrong (Keith, 1947). Geochronologists, including the authors of this contribution, would do well to have a similar attitude. If there is one thing that can be learned from 100 years of research into Taung, then it is that scientific progress is not always linear. The solution of the riddle of human evolution will require humility and a lot of patience.

Acknowledgments

The ID-TIMS measurements for TDPH14 were carried out by Steve Noble, with $^{234}U/^{238}U$-measurements provided by Vanessa Pashley. This work was funded through NERC Standard Grant NE/T001518/1 awarded to PV, National Geographic grants #8774-10 and #3212 awarded to PH, a NERC Isotope Facilities Grant (IP-1489-1114) awarded to PH and a NERC Small Grant NE/H011102/1 awarded to RP. The authors are grateful for insightful reviews by Darryl Granger, David Richards and an anonymous reviewer; and for numerous editorial suggestions from Bernard Wood.

References

Alemseged, Z., Wynn, J. G., Kimbel, W. H., Reed, D., Geraads, D., and Bobe, R. A new hominin from the Basal Member of the Hadar Formation, Dikika, Ethiopia, and its geological context. *Journal of Human Evolution*, 49(4):499–514, 2005.

Asfaw, B., White, T., Lovejoy, O., Latimer, B., Simpson, S., and Suwa, G. *Australopithecus garhi*: a new species of early hominid from Ethiopia. *Science*, 284(5414):629–635, 1999.

Berger, L. R. A preliminary estimate of the age of the Gladysvale australopithecine site. *Palaeontologia Africana*, 1993.

Berger, L. R. and Hawks, J. Australopithecus prometheus is a nomen nudum. *American Journal of Physical Anthropology*, 168(2):383–387, 2019.

Berger, L. R., Keyser, A. W., and Tobias, P. V. Gladysvale: first early hominid site discovered in South Africa since 1948. *American Journal of Physical Anthropology*, 92(1):107–111, 1993.

Bruxelles, L., Stratford, D. J., Maire, R., Pickering, T. R., Heaton, J. L., Beaudet, A., Kuman, K., Crompton, R., Carlson, K. J., Jashashvili, T., et al. A multiscale stratigraphic investigation of the context of StW 573 'Little Foot'and Member 2, Sterkfontein Caves, South Africa. *Journal of Human Evolution*, 133:78–98, 2019.

Clarke, R. J. and Kuman, K. The skull of StW 573, a 3.67 ma Australopithecus prometheus skeleton from Sterkfontein Caves, South Africa. *Journal of Human Evolution*, 134:102634, 2019.

paper	site	sample	age	$\left[^{234}U/^{238}U\right]_i$	$\left[^{234}U/^{238}U\right]_m$
Walker et al. (2006)	Sterkfontein	STA09	2.17	2.92*	1.0043
Walker et al. (2006)	Sterkfontein	STA12	2.11	2.62*	1.0043
Walker et al. (2006)	Sterkfontein	STA15	2.24	3.34*	1.0043
Walker et al. (2006)	Sterkfontein	SKA3	2.25	3.41*	1.0043
Dirks et al. (2010)	Malapa	NHL09	2.026	4.12*	1.0103
Pickering et al. (2019)	Coopers's cave	CD-1	1.38	2.22	1.0248
Pickering et al. (2019)	Bolt's farm	WP-160-1	2.78	6.48*	1.0022
Pickering et al. (2019)	Bolt's farm	WP-160-2	2.269	8.186	1.0119
Pickering et al. (2019)	Bolt's farm	BFMC-1	1.776	1.95*	1.0064
Pickering et al. (2019)	Bolt's farm	BFMC-6	1.383	1.901	1.0182
Pickering et al. (2019)	Bolt's farm	AV01	2.41	4.232	1.0036
Pickering et al. (2019)	Bolt's farm	AV03	2.668	9.46*	1.0046
Pickering et al. (2019)	Bolt's farm	WP-160-6L	1.752	2.011	1.0072
Pickering et al. (2019)	Drimolen	DN26	1.889	2.652	1.0078
Pickering et al. (2019)	Drimolen	DN09	1.789	1.789	1.0050
Pickering et al. (2019)	Drimolen	DN39-A	2.673	5.971	1.0025
Pickering et al. (2019)	Drimolen	DMK5	2.664	5.336	1.0023
Pickering et al. (2019)	Haasgat	HG1	1.686	7.03	1.0508
Pickering et al. (2019)	Hoogland	HL1	3.145	12.879	1.0016
Pickering et al. (2019)	Malapa	M6	2.048	3.51	1.0065
Pickering et al. (2019)	Malapa	M1_1	2.026	4.11*	1.0103
Pickering et al. (2019)	Sterkfontein	OE14	2.03	4.739	1.0119
Pickering et al. (2019)	Sterkfontein	OE13	1.784	2.558	1.0099
Pickering et al. (2019)	Sterkfontein	1/8	2.8	5.515	1.0016
Pickering et al. (2019)	Sterkfontein	4/9	2.645	2.578	1.0009
Pickering et al. (2019)	Sterkfontein	1/15	2.747	5.301	1.0018
Pickering et al. (2019)	Sterkfontein	SB1	2.347	3.32	1.0031
Pickering et al. (2019)	Swartkrans	SWK-5	1.8	6.756	1.0352
Pickering et al. (2019)	Swartkrans	SWK-7	2.248	2.555	1.0027
Pickering et al. (2019)	Swartkrans	SWK-9	1.706	2.237	1.0098
Pickering et al. (2019)	Swartkrans	SWK-12	2.249	4.824	1.0065

Table 1: The underlying data for Figure 3. Asterisks mark $\left[^{234}U/^{238}U\right]_i$-values inferred from the $\left[^{234}U/^{238}U\right]_m$-values. Other values are reproduced exactly as reported in the papers.

$X = \frac{^{238}U}{^{206}Pb}$	$s[X]\,(\%)$	$Y = \frac{^{207}Pb}{^{206}Pb}$	$s[Y]\,(\%)$	$Z = \frac{^{204}Pb}{^{206}Pb}$	$s[Z]\,(\%)$	$r[X,Y]$	$r[X,Z]$	$r[Y,Z]$
1473	0.59	0.24	1.52	0.0133	1.8	-0.996	-0.974	0.9892
1757	1.09	0.13	6.19	0.0059	9.1	-0.998	-0.995	0.9993
1784	0.76	0.11	5.24	0.0045	8.5	-0.995	-0.991	0.9992
1330	0.77	0.31	1.38	0.0179	1.6	-0.998	-0.962	0.9708

Table 2: ID-TIMS U–Pb data for Figure 6. Note the strong error correlations, which are caused by the blank correction (Schmitz and Schoene, 2007).

Dart, R. A. Australopithecus africanus the man-ape of South Africa. *Nature*, 115(2884):195–199, 1925.

Deino, A. L., Gibert, L., and Vidal, C. M. Using Radiometric Dating, Magnetostratigraphy, and Tephrostratigraphy to Calibrate Rates of Hominin Evolution in the East African Rift. *Elements*, 19(2):88–95, 2023.

Dirks, P. H., Kibii, J. M., Kuhn, B. F., Steininger, C., Churchill, S. E., Kramers, J. D., Pickering, R., Farber, D. L., Mériaux, A.-S., Herries, A. I., et al. Geological setting and age of Australopithecus sediba from southern Africa. *Science*, 328(5975):205–208, 2010.

Engel, J., Woodhead, J., Hellstrom, J., Maas, R., Drysdale, R., and Ford, D. Corrections for initial isotopic disequilibrium in the speleothem U-Pb dating method. *Quaternary Geochronology*, 54: 101009, 2019.

Frost, S. R., White, F. J., Reda, H. G., and Gilbert, C. C. Biochronology of South African hominin-bearing sites: A reassessment using cercopithecid primates. *Proceedings of the National Academy of Sciences*, 119(45):e2210627119, 2022.

Granger, D. E., Gibbon, R. J., Kuman, K., Clarke, R. J., Bruxelles, L., and Caffee, M. W. New cosmogenic burial ages for Sterkfontein member 2 Australopithecus and member 5 Oldowan. *Nature*, 522(7554):85–88, 2015.

Granger, D. E., Stratford, D., Bruxelles, L., Gibbon, R. J., Clarke, R. J., and Kuman, K. Cosmogenic nuclide dating of Australopithecus at Sterkfontein, South Africa. *Proceedings of the National Academy of Sciences*, 119(27):e2123516119, 2022.

Grün, R. and Stringer, C. Direct dating of human fossils and the ever-changing story of human evolution. *Quaternary Science Reviews*, 322:108379, 2023.

Herries, A. I. and Shaw, J. Palaeomagnetic analysis of the Sterkfontein palaeocave deposits: Implications for the age of the hominin fossils and stone tool industries. *Journal of human evolution*, 60(5):523–539, 2011.

Hopley, P. J. and Kuhn, B. F. The Paleoecology of the Australopithecus africanus Type Site at Taung, South Africa. In S.C., R. and Bobe, R., editors, *African Paleoecology and Human Evolution*, pages 135–141. Cambridge University Press, 2022.

Hopley, P. J., Marshall, J. D., Weedon, G. P., Latham, A. G., Herries, A. I., and Kuykendall, K. L. Orbital forcing and the spread of C4 grasses in the late Neogene: stable isotope evidence from South African speleothems. *Journal of Human Evolution*, 53(5):620–634, 2007.

Hopley, P. J., Herries, A. I., Baker, S. E., Kuhn, B. F., and Menter, C. G. Brief communication: beyond the South African cave paradigm –Australopithecus Africanus from Plio-Pleistocene paleosol deposits at Taung. *American Journal of Physical Anthropology*, 151(2):316–324, 2013.

Hopley, P. J., Reade, H., Parrish, R., De Kock, M., and Adams, J. W. Speleothem evidence for C3 dominated vegetation during the Late Miocene (Messinian) of South Africa. *Review of Palaeobotany and Palynology*, 264:75–89, 2019.

Hopley, P. and Maxwell, S. J. Environmental and stratigraphic bias in the Hominin Fossil Record: implications for theories of the climatic forcing of human evolution. In SC, R. and R, B., editors, *African Paleoecology and Human Evolution*, pages 15–23. Cambridge University Press, 2022.

Hrdlčka, A. The Taungs ape. *American Journal of Physical Anthropology*, 8(4):379, 1925.

Isaac, G. L. Sorting out the muddle in the middle: an anthropologist's post-conference appraisal. *After the australopithecines*, pages 875–887, 1975.

Ivanovich, M. Uranium series disequilibrium: concepts and applications. *Radiochimica Acta*, 64 (2):81–94, 1994.

Keith, A. Australopithecinae or Dartians. *Nature*, 159(4037):377–377, 1947.

Kramers, J. D. and Dirks, P. H. The age of fossil StW573 ('Little Foot'): An alternative interpretation of $^{26}Al/^{10}Be$ burial data. *South African Journal of Science*, 113(3-4):1–8, 2017.

Kronfeld, J., Vogel, J., and Talma, A. A new explanation for extreme $^{234}U/^{238}U$ disequilibria in a dolomitic aquifer. *Earth and Planetary Science Letters*, 123(1-3):81–93, 1994.

Kuhn, B. F., Carlson, K. J., Hopley, P. J., Zipfel, B., and Berger, L. R. Identification of fossilized eggshells from the Taung hominin locality, Taung, Northwest Province, South Africa. *Palaeontologia electronica*, 18(1):1–16, 2015.

Leakey, L., Evernden, J., and Curtis, G. Age of Bed I, Olduvai Gorge, Tanganyika. *Nature*, 191 (4787):478–479, 1961.

Li, Y. and Vermeesch, P. Inverse isochron regression for Re–Os, K–Ca and other chronometers. *Geochronology*, 3(2):415–420, 2021.

Ludwig, K. R. On the treatment of concordant uranium-lead ages. *Geochimica et Cosmochimica Acta*, 62:665–676, 1998. doi: 10.1016/S0016-7037(98)00059-3.

Maguire, J. M. Recent geological, stratigraphic and palaeontological studies at Makapansgat Limeworks. In *Late Cainozic palaeoclimates of the Southern Hemisphere. International symposium held by the South African Society for Quaternary Research; Swaziland*, pages 151–164, 1984.

Makhubela, T. V. and Kramers, J. D. Testing a new combined (U, Th)–He and U/Th dating approach on Plio-Pleistocene calcite speleothems. *Quaternary Geochronology*, 67:101234, 2022.

Maxwell, S. J., Hopley, P. J., Upchurch, P., and Soligo, C. Sporadic sampling, not climatic forcing, drives observed early hominin diversity. *Proceedings of the National Academy of Sciences*, 115 (19):4891–4896, 2018.

McKee, J. K. Faunal dating of the Taung hominid fossil deposit. *Journal of Human Evolution*, 25 (5):363–376, 1993.

McKee, J. K. Return to the Taung cave paradigm. *American Journal of Physical Anthropology*, 159(2):348–351, 2016.

McKee, J. K. and Tobias, P. V. Taung stratigraphy and taphonomy: preliminary results based on the 1988–93 excavations. *South African Journal of Science*, 90(4):233–235, 1994.

McLean, N. M., Smith, C. J. M., Roberts, N. M. W., and Richards, D. A. Connecting the U-Th and U-Pb Chronometers: New Algorithms and Applications. *AGU Fall Meeting Abstracts*, December 2016.

Mongle, C. S., Pugh, K. D., Strait, D. S., and Grine, F. E. Modelling hominin evolution requires accurate hominin data. *Nature Ecology & Evolution*, 6(8):1090–1091, 2022.

Parker, J. F., Hopley, P. J., and Kuhn, B. F. Fossil carder bee's nest from the hominin locality of Taung, South Africa. *Plos one*, 11(9):e0161198, 2016.

Parrish, R. R., Parrish, C. M., and Lasalle, S. Vein calcite dating reveals Pyrenean orogen as cause of Paleogene deformation in southern England. *Journal of the Geological Society*, 175(3): 425–442, 2018.

Partridge, T. C., Granger, D. E., Caffee, M. W., and Clarke, R. J. Lower Pliocene hominid remains from Sterkfontein. *Science*, 300(5619):607–612, 2003.

Peabody, F. E. Travertines and cave deposits of the Kaap Escarpment of South Africa, and the type locality of Australopithecus *africanus* Dart. *Geological Society of America Bulletin*, 65(7): 671–706, 1954.

Pickering, R. and Kramers, J. D. Re-appraisal of the stratigraphy and determination of new U-Pb dates for the Sterkfontein hominin site, South Africa. *Journal of Human Evolution*, 59(1):70–86, 2010.

Pickering, R., Dirks, P. H., Jinnah, Z., De Ruiter, D. J., Churchill, S. E., Herries, A. I., Woodhead, J. D., Hellstrom, J. C., and Berger, L. R. *Australopithecus sediba* at 1.977 Ma and implications for the origins of the genus *Homo*. *Science*, 333(6048):1421–1423, 2011.

Pickering, R., Jacobs, Z., Herries, A. I., Karkanas, P., Bar-Matthews, M., Woodhead, J. D., Kappen, P., Fisher, E., and Marean, C. W. Paleoanthropologically significant South African sea caves dated to 1.1–1.0 million years using a combination of U–Pb, TT-OSL and palaeomagnetism. *Quaternary Science Reviews*, 65:39–52, 2013.

Pickering, R., Herries, A. I., Woodhead, J. D., Hellstrom, J. C., Green, H. E., Paul, B., Ritzman, T., Strait, D. S., Schoville, B. J., and Hancox, P. J. U–Pb-dated flowstones restrict South African early hominin record to dry climate phases. *Nature*, 565(7738):226, 2019.

Püschel, H. P., Bertrand, O. C., O'reilly, J. E., Bobe, R., and Püschel, T. A. Divergence-time estimates for hominins provide insight into encephalization and body mass trends in human evolution. *Nature ecology & evolution*, 5(6):808–819, 2021.

Reed, K. E., Kuykendall, K. L., Herries, A. I., Hopley, P. J., Sponheimer, M., and Werdelin, L. Geology, Fauna, and Paleoenvironmental Reconstructions of the Makapansgat Limeworks Australopithecus africanus-Bearing Paleo-Cave. *African Paleoecology and Human Evolution. Cambridge University, Cambridge*, pages 66–81, 2022.

Richards, D. A., Bottrell, S. H., Cliff, R. A., Ströhle, K., and Rowe, P. J. U-Pb dating of a speleothem of Quaternary age. *Geochimica et Cosmochimica Acta*, 62(23-24):3683–3688, 1998.

Schmitz, M. D. and Schoene, B. Derivation of isotope ratios, errors, and error correlations for U-Pb geochronology using ^{205}Pb-^{235}U-(^{233}U)-spiked isotope dilution thermal ionization mass spectrometric data. *Geochemistry, Geophysics, Geosystems*, 8(8), 2007.

Schwarcz, H. P., Grün, R., and Tobias, P. V. ESR dating studies of the australopithecine site of Sterkfontein, South Africa. *Journal of Human Evolution*, 26(3):175–181, 1994.

Tobias, P. V. Implications of the new age estimates of the early South African hominids. *Nature*, 246(5428):79–83, 1973.

Tobias, P. V. The Fossil Hominids. In Partridge, T. and Maud, R., editors, *The Cenozoic of Southern Africa*, Oxford monographs on geology and geophysics, chapter 17, page 252–276. Oxford University Press, 2000.

Tobias, P. V. Dart, Taung, and the "missing link": an essay on the life and work of Emeritus Professor Raymond Dart, based on a tribute to Professor Dart on his 90$^{\text{th}}$ birthday, delivered at the University of the Witwatersrand, Johannesburg, on 22 June 1983. *(No Title)*, 1984.

Tobias, P. V., Vogel, J. C., Oschadleus, H. D., Partridge, T. C., and McKee, J. K. New isotopic and sedimentological measurements of the Thabaseek deposits (South Africa) and the dating of the Taung hominid. *Quaternary Research*, 40(3):360–367, 1993.

Vaks, A., Mason, A., Breitenbach, S., Kononov, A., Osinzev, A., Rosensaft, M., Borshevsky, A., Gutareva, O., and Henderson, G. Palaeoclimate evidence of vulnerable permafrost during times of low sea ice. *Nature*, 577(7789):221–225, 2020.

van Holstein, L. A. and Foley, R. A. A process-based approach to hominin taxonomy provides new perspectives on hominin speciation. *Evolutionary Anthropology: Issues, News, and Reviews*, 31 (4):166–174, 2022.

van Holstein, L. A. and Foley, R. A. Diversity-dependent speciation and extinction in hominins. *Nature Ecology & Evolution*, pages 1–11, 2024.

Vermeesch, P., Balco, G., Blard, P.-H., Dunai, T. J., Kober, F., Niedermann, S., Shuster, D. L., Strasky, S., Stuart, F. M., Wieler, R., et al. Interlaboratory comparison of cosmogenic ^{21}Ne in quartz. *Quaternary Geochronology*, 2012. doi: 10.1016/j.quageo.2012.11.009.

Vogel, J. and Partridge, T. Preliminary radiometric ages for the Taung tufas. In *Late Cainozic palaeoclimates of the Southern Hemisphere. International symposium held by the South African Society for Quaternary Research; Swaziland*, pages 507–514, 1984.

Walker, J. *Uranium-Lead dating of Hominid fossil sites in South Africa.* PhD thesis, University of Leeds, 2005.

Walker, J., Cliff, R. A., and Latham, A. G. U-Pb isotopic age of the StW 573 hominid from Sterkfontein, South Africa. *Science*, 314(5805):1592–1594, 2006.

Wood, B. and K. Boyle, E. Hominin taxic diversity: Fact or fantasy? *American journal of physical anthropology*, 159:37–78, 2016.

Woodhead, J. and Pickering, R. Beyond 500 ka: Progress and prospects in the UPb chronology of speleothems, and their application to studies in palaeoclimate, human evolution, biodiversity and tectonics. *Chemical Geology*, 322:290–299, 2012.